Phase-matched second-harmonic generation in planar waveguides

G. Marowsky,* E. J. Canto-Said, S. Lehmann, and F. Sieverdes
Max-Planck-Institut für Biophysikalische Chemie, Abteilung Laserphysik, Am Fassberg, D-37077 Göttingen, Germany

A. Bratz
Rheinisch-Westfälische Technische Hochschule Aachen, Templergraben 55, D-52062 Aachen, Germany
(Received 28 June 1993)

Second-harmonic generation exploiting evanescent field interaction has been investigated for a planar dielectric waveguide covered with a thin organic layer. The coherent nature of the frequency-doubling process in such a structure was studied experimentally by systematic ablation of the nonlinear film in an *in situ* setup. An increase in the conversion efficiency by two orders of magnitude has been observed for a nonoptimized second-order susceptibility of the coverage layer.

I. INTRODUCTION

The use of waveguiding structures for frequency conversion of the radiation from low-power lasers has attracted considerable scientific and technical interest in the last few years. Various proposals for practical realizations and a number of theoretical studies have been published.[1–4] The use of waveguiding structures should permit long interaction lengths at high optical intensities to facilitate frequency conversion by nonlinear-optical processes. The modal dispersion of waveguides provides an additional parameter with which to achieve phase matching, which is generally realized by continuous periodic modulation of the linear and/or nonlinear properties of the guiding structure.[5,6] The organics in thin films are widely considered to be promising candidates for layered frequency conversion devices, owing to their extremely high second-order nonlinearity.[7] We are studying quasi-phase-matched second-harmonic generation (SHG) by incorporating a periodic structure into a planar, linear waveguide configuration. Rather than applying a periodically domain-inverted nonlinear waveguide, we use a linear, lossless, commercial waveguide covered with a periodically structured nonlinear organic adsorbate.

II. THEORY

The basic theory of guided waves in planar structures and frequency conversion by various nonlinear optical materials present in such structures has been discussed by several authors.[8–11] In this paper we shall follow the formalism of Ref. 9, and hence only a brief summary of the relevant equations is given. In a planar optical waveguide covered with a thin film of organic molecules, the field in the cover material is exponentially damped and excites a surface polarization in the adsorbate which is the source of radiation at frequency 2ω. Due to modal dispersion, the two waves inside the waveguide will travel at different velocities that can be characterized by the effective guide indices of refraction n_{eff} at the two frequencies.[12] The quantity n_{eff} is defined by the ration β/k, with β the propagation constant in the direction of propagation x, and k that of free space ($k=\omega/c$). Various methods have been proposed in the past to compensate for the concomitant phase mismatch.[9,13,14] It is now well established that periodic structuring can provide quasi-phase-matching for long interaction lengths limited only by the pump depletion or the increasing losses for both waves due to scattering and absorption.[15] In Refs. 9 and 14 it has been shown in detail how the necessary grating period l_g can be derived from propagation considerations for both fundamental and second-harmonic waves *inside* the dispersive waveguide carrying a nonlinear, periodically modulated surface polarization in the plane $z=z_0$ (cf. Fig. 1). It should be noted that this "polarization sheet"[16] is located *outside* the waveguiding structure, and hence frequency conversion can occur only via evanescent field interaction. According to Ref. 9, the grating period l_g, which optimizes the frequency conversion between two selected modes k and k' of frequencies ω and 2ω, respectively, results from a Fourier transformation of the x-dependent surface susceptibility $\chi^{(2)}_{S,\text{eff}}(x)$ and consideration of those Fourier amplitudes that optimize the

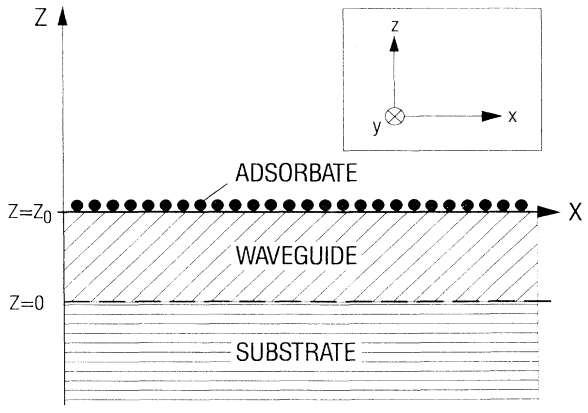

FIG. 1. System of coordinates x, y, and z of the waveguiding structure considered together with the schematic thin-film adsorbate located at $z=z_0$.

conversion. The nonlinear surface polarization can be written as usual as

$$\mathbf{P}_S^{(2\omega)}(x)=\chi_{S,\text{eff}}^{(2)}(x)\mathbf{E}^{(\omega)}(x,z_0)\mathbf{E}^{(\omega)}(\mathbf{x},\mathbf{z}_0)\ . \tag{1}$$

Equation (1) describes the tensorial product of susceptibility and fundamental field amplitudes $\mathbf{E}^{(\omega)}(\mathbf{x},\mathbf{z}_0)$ taken at the position of the polarization sheet, $z=z_0$. The susceptibility $\chi_{S,\text{eff}}^{(2)}(x)$ can be split into an x-independent contribution $\chi_S^{(2)}$ and a periodic function $g(x)$, with

$$\chi_{S,\text{eff}}^{(2)}\equiv\chi_S^{(2)}g(x)\ . \tag{2}$$

The actual shape of $g(x)$ will be discussed in more detail in Sec. III. Let us now define the required Fourier amplitudes by

$$\hat{\mathbf{P}}_S^{(2\omega)}(\beta_j)\propto\hat{\mathbf{g}}(\beta_j)=\frac{1}{2\pi}\int g(x)e^{-\beta_j x}dx\ . \tag{3}$$

The index j in Eq. (2) reflects the fact that we are considering guided modes only and hence the amplitudes $\hat{\mathbf{g}}(\beta_j)$ will have only discrete values for the selected modes of index j. For conversion of a fundamental mode at frequency ω, with propagation constant β_k into its harmonic with propagation constant $\beta_{k'}$, the Fourier amplitude $\hat{\mathbf{g}}(2\beta_k-\beta_{k'})$ that needs to be optimized can be written as

$$\hat{\mathbf{g}}(2\beta_k-\beta_{k'})=\frac{1}{2\pi}\int_{-\infty}^{+\infty}g(x)e^{i(2\beta_k-\beta_{k'})x}dx\ . \tag{4}$$

The magnitude of this expression can be written as

$$|\hat{\mathbf{g}}(\Delta\beta)|=\frac{|e^{i\Delta\beta b}-1|}{|2\pi i\Delta\beta|}\frac{\sin(N\Delta\beta l_g/2)}{\sin(\Delta\beta l_g/2)}\ , \tag{5}$$

with $\Delta\beta=2\beta_k-\beta_{k'}$. The right-hand side of the last equation will be a maximum whenever $b=l_g/2$—hence 50% per grating period l_g are covered with the SH-active layer—and

$$l_g=\frac{2\pi}{2\beta_k-\beta_{k'}}=\frac{\lambda}{2}\frac{1}{|n_{k'}^{(2\omega)}-n_k^{(\omega)}|}\ , \tag{6}$$

with λ the wavelength of the fundamental, and $n_{k'}^{(2\omega)}$ and $n_k^{(\omega)}$ the respective effective guide indices. It should be noted that Eq. (6) is completely analogous to the expression for the coherence length l_c encountered in *bulk* second-harmonic generation:[17]

$$l_c=\frac{\lambda}{2}\frac{1}{|n^{(2\omega)}-n^{(\omega)}|}\ . \tag{7}$$

The only difference between Eqs. (6) and (7) is the fact that waveguiding frequency conversion devices should make use of the *effective* indices of refraction. Under (quasi)-phase-matched conditions ($l_g\equiv l_c$) the SH output will increase quadratically with the total device length $L=ml_g$, where m denotes the number of grating periods. The result of Eq. (6) may be interpreted as follows: due to the different phase velocities of the ω and 2ω modes inside the waveguide there is a periodical increase and decrease of the SH intensity along the propagation direction. The periodical structuring of the adsorbate yields a nonlinear grating where destructive contributions of the nonlinear polarization are suppressed. The result of Eq. (6) offers new approaches to achieving phase matching, which make the guided-wave configurations—in addition to their long-range intensity confinement—so attractive for any nonlinear-optical frequency conversion scheme.

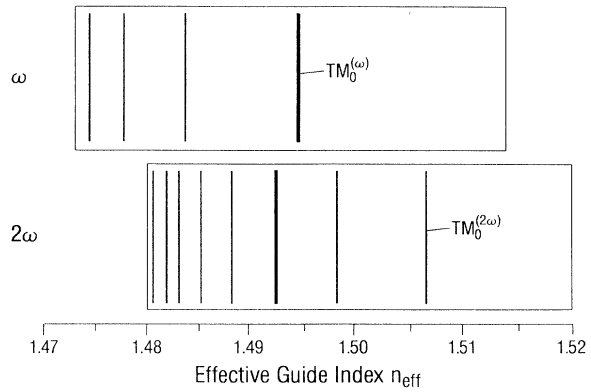

FIG. 2. Compilation of TM$_k^{(\omega)}$- and TM$_{k'}^{(2\omega)}$-mode spectra vs the effective guide index n_{eff} for the waveguide configuration considered in Sec. III.

(i) The introduction of the effective guide index allows the use of different geometrical schemes[12] for the achievement of $l_c\to\infty$ or $n_{k'}^{(2\omega)}=n_k^{(\omega)}$.

(ii) One can search for accidental coincidences in the effective guide index or tune the fundamental wavelength appropriately to achieve *perfect* phase matching[18] for an adjacent mode pair.

In Sec. III we shall consider only conversion between transverse electromagnetic (TM) modes. The mode spectra in Fig. 2 are the effective guide indices for modes at both frequencies for the waveguide used in the experiments. It should be pointed out that $\omega\to2\omega$ conversion for adjacent modes is most efficient. Normalizing all conversion efficiencies to unity for TM$_0^{(\omega)}\to$TM$_0^{(2\omega)}$ conversion results in the efficiencies for both TM$_0^{(\omega)}$ and TE$_0^{(\omega)}$ excitations which are shown in Table I. It is obvious from this table that TM$_k^{(\omega)}\to$TM$_{k'}^{(2\omega)}$ conversions are always more efficient than TE$_0^{(\omega)}\to$TM$_{k'}^{(2\omega)}$ conversions. This is simply a consequence of the fact that second-harmonic generation with p-polarized input and p-polarized output at frequency 2ω is generally more efficient than pure s-polarized excitation—irrespective of how large the relevant susceptibility component $\chi_{zyy}^{(2)}$ is in

TABLE I. Normalized efficiencies for both TM$_0^{(\omega)}$ and TE$_0^{(\omega)}$ excitation of the first six TM$_{k'}^{(2\omega)}$ modes. TM$_0^{(\omega)}\to$TM$_0^{(2\omega)}$ efficiency is set to unity.

TM$_{k'}^{(2\omega)}$	TE$_0^{(\omega)}$-exc.	TM$_0^{(\omega)}$-exc.
0	0.040	1.00
1	0.031	0.78
2	0.025	0.61
3	0.019	0.48
4	0.015	0.37
5	0.011	0.27

the latter case. In addition, it should be noted that there exists no $TE_0^{(\omega)} \rightarrow TE_{k'}^{(2\omega)}$ conversion for isotropic coverage films due to the absence of anisotropic components such as $\chi_{yyy}^{(2)}$.

III. EXPERIMENT

The experimental setup shown in Fig. 3 was designed to convert different modes $TM_k^{(\omega)}$ of the fundamental, selected by the input angle Θ_i, into output modes $TM_{k'}^{(2\omega)}$ at frequency 2ω upon variation of the acceptance angle Θ_a. The detection side consisted of a monochromator-multiplier combination equipped with a photon-counting system for signal registration. Polarizers P_1 and P_2 served to characterize the respective polarization conditions. The adsorbate could be ablated *in situ* by the focused radiation of a frequency-doubled Nd:YAG (yttrium aluminum garnet) laser. This laser, delivering 100-mJ pulses of 10-ns duration at 532 nm allowed ablation of the nonlinear organic material in 10-μm steps. Laser ablation was also used to determine the coherence length l_c of the waveguide-adsorbate configuration, and subsequently to produce the necessary grating which could be inspected by SH microscopy.[14] The laser shown in Fig. 3 was a mode-locked and Q-switched Nd:YAG laser delivering pulses of 70-ps duration and 125-kW peak power at its fundamental wavelength of 1064 nm. Prism coupling was used for the input of the fundamental and for extraction of the optical harmonic at 532 nm. The waveguide carrying the nonlinear adsorbate had an exponential refractive index profile, as shown in Fig. 4 with $n_s = 1.4798$, $\Delta n = 0.04$, and a decay constant $\alpha = (3.6\ \mu\text{m})^{-1}$ according to the manufacturer's specifications.[19] All index data refer to 532 nm. The nonlinear film itself was 100 μm thick, prepared by simply dipping the waveguide under reproducible conditions[20] into a poly(methyl)methacrylate (PMMA) chloroform solution with addition of a hemicyanine dye of high second-order nonlinearity.[21] The resulting adsorbates were of excellent homogeneity and easy to ablate, but of relatively low susceptibility due to the random orientation of the chromophores at the glass-polymer interface. The nonlinear surface susceptibility $\chi_S^{(2)}$ was measured independently in total internal reflection geometry.[22] The dominant contribution to $\chi_S^{(2)}$ was found to be $\chi_{zzz}^{(2)} \approx 10^{-16}$ esu for a 5×10^{-4} molar dye-polymer solution after evaporation of the solvent. The conversion efficiency considerations will be based on this experimentally obtained susceptibility value.

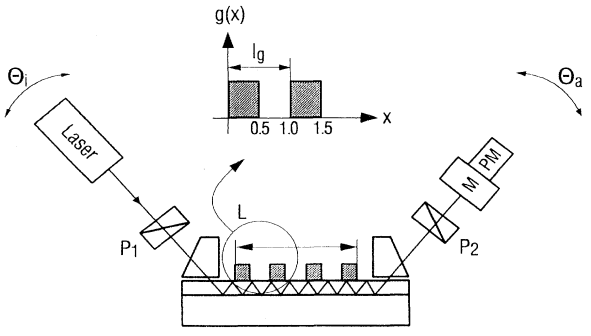

FIG. 3. Experimental setup of a linear waveguide carrying a periodically structured nonlinear adsorbate of length $L = ml_g$. Inset shows magnified details of a susceptibility distribution as introduced in Eq. (2).

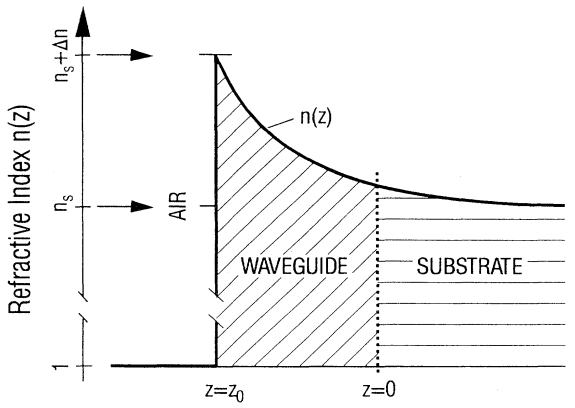

FIG. 4. z dependence of the refractive index $n(z)$ supporting the TM modes shown in Fig. 2. The nonlinear adsorbate located at $z = z_0$ has not been shown for the sake of simplicity.

IV. RESULTS AND DISCUSSION

A. Coherence length

In order to increase the conversion efficiency of the proposed waveguide configuration, periodic patterning must be performed to achieve quasi-phase-matching. As already explained in Sec. II, the grating period must match the coherence length l_c according to Eq. (6). Again $TM_k^{(\omega)} \rightarrow TM_{k'}^{(2\omega)}$ conversion will be only considered. In the absence of any phase-matching efforts, we expect a sinusoidal oscillation of the SH intensity with the coherence length l_c upon variation of the adsorbate length. The particular value of l_c will depend on the selected mode pair $TM_k^{(\omega)}$ and $TM_{k'}^{(2\omega)}$. The excitation of a waveguide carrying an unstructured adsorbate resulted in the emission of up to four SH modes, as shown in the photograph of Fig. 5. Both the respective acceptance an-

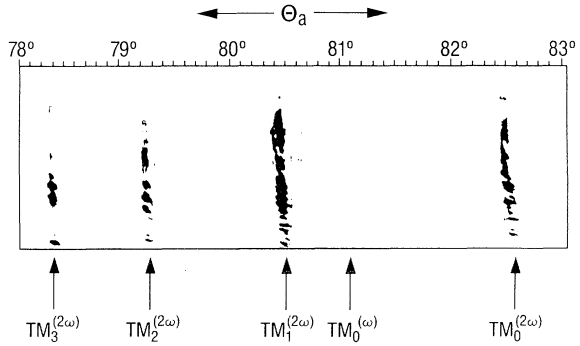

FIG. 5. SH modes $TM_0^{(2\omega)}, \ldots, TM_3^{(2\omega)}$ upon variation of the acceptance angle Θ_a between 78° and 83°. Also indicated is the angular position of the fundamental mode $TM_0^{(\omega)}$.

gle Θ_a as well as the (invisible) position of the exciting fundamental $TM_0^{(\omega)}$ mode are shown in the figure. For the photographic registration, the mode spectrum emerging from the waveguide with the unstructured adsorbate was recorded with an exposure time of 15 s. The increased sensitivity of the photon-counting detection system directed to a selected $TM_{k'}^{(2\omega)}$ mode should allow the observation of oscillations with the coherence length upon ablation of the coverage. Figure 6 shows the experimentally obtained beat patterns for $TM_0^{(\omega)}$-excited $TM_1^{(2\omega)}$, $TM_2^{(2\omega)}$, and $TM_3^{(2\omega)}$ modes. The dashed lines represent the recorded SH intensity upon ablation of the adsorbate in 10-μ steps—the solid line is a Fourier fit to the *experimental* coherence length values $l_c^{(e)}$, which are also indicated at each pattern. We attribute the obvious deviations from the theoretical values given in the figure caption—using the *unperturbed* index profile $n(z)$ only—to the influence of the linear-optical properties of the 100-μm-thick polymer coverage. Consequently we shall rely on the experimental $l_c^{(e)}$ values rather than using the calculated *theoretical* coherence length data. Inspection of Fig. 6 suggests that signal-to-noise ratio considerations make the $TM_0^{(\omega)} \rightarrow TM_2^{(2\omega)}$ conversion most attractive for an actual quasi-phase-matching experiment. The beat patterns of Fig. 6 when observed in a planar waveguide configuration correspond to the well-known phenomenon of bulk phase mismatch between the fundamental and harmonic waves in nonlinear crystals, namely, maker fringes.[23]

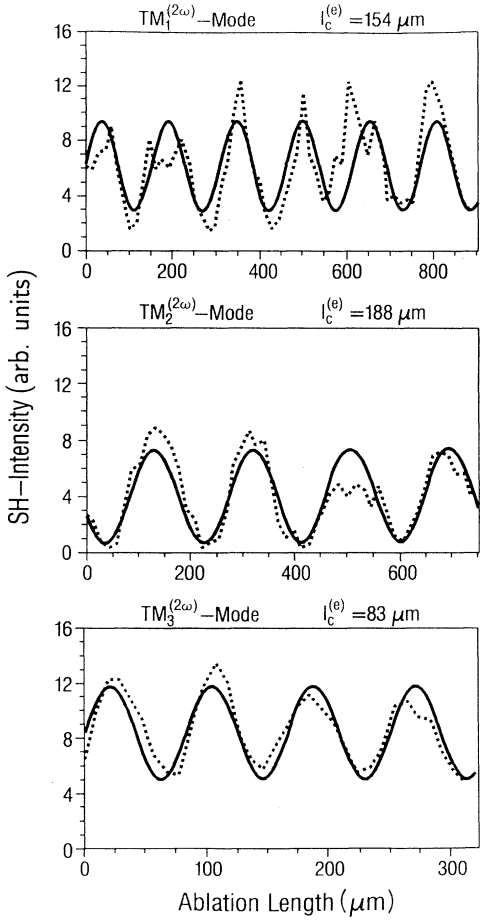

FIG. 6. Variations in SH intensity with ablation length for three selected SH modes. Experimentally determined coherence lengths $l_c^{(e)}$ are indicated. Taking into account the diffusion-controlled index profile $n(z)$ shown in Fig. 4 resulted in $l_c = 142$ ($TM_1^{(2\omega)}$ excitation), 174 ($TM_2^{(2\omega)}$ excitation), and 67 μm ($TM_3^{(2\omega)}$ excitation).

B. Phase matching

Based upon the experimental results of Sec. IV A for the coherence length of the $TM_0^{(\omega)} \rightarrow TM_2^{(2\omega)}$ conversion with $l_c^{(e)} = 188$ μm, we have studied the properties of quasi-phase-matched SH emission as to mode selectivity and length dependence. Figures 7 and 8 summarize the experimental results. The necessary *in situ* ablation technique allowed reproducible patterning of up to 20 grating periods, corresponding to a total structured adsorbate length of 20×188 μm $\hat{=}$ 3.8 mm. As compared to the unstructured adsorbate, the intensity of the selected $TM_2^{(2\omega)}$ mode could be enhanced by more than a factor of 100. Figure 7 shows that other non-phase-matched modes are still present. By a direct measurement of the respective powers P_ω and $P_{2\omega}$ emerging from the waveguide, an experimental conversion efficiency $\eta^{(e)} = P_{2\omega}/P_\omega^2 = 1.1 \times 10^{-10}$ was determined for this total grating length of 3.8 mm and $P_\omega = 25$ kW. Based upon the independently determined susceptibility value, a conversion efficiency $\eta^{(t)}$ of 3.5×10^{-10} was expected under the above-mentioned experimental conditions for the selected mode pair. Taking into account the various uncertainties entering the theoretical efficiency calculation, such as the precise knowledge of the index profile $n(z)$ for the determination of the field strength $\mathbf{E}^{(\omega)}(\mathbf{z}_0)$ of the fundamental mode at the position of the adsorbate, or the problems associated with a precise second-order susceptibility measurement, the agreement between $\eta^{(t)}$ and $\eta^{(e)}$ is surprising despite a deviation by a factor of 3. Even without changing the susceptibility $\chi_S^{(2)}$ itself, the conversion efficiency of the device can be increased immediately by nearly two orders of magnitude by removing only 50% of the adsorbate per grating period (instead of the currently

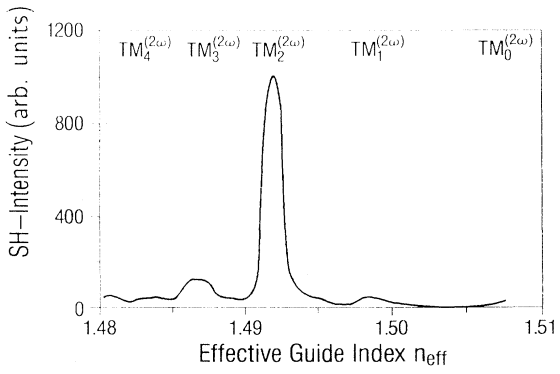

FIG. 7. SH intensity vs the effective guide index upon mode-selective phase matching of the $TM_0^{(\omega)} \rightarrow TM_2^{(2\omega)}$ conversion.

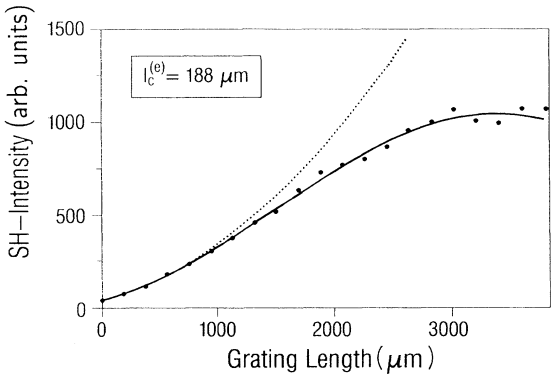

FIG. 8. SH intensity vs the length of a periodically structured nonlinear adsorbate, showing a strong deviation from the expected square dependence.

70%) for optimized operation, and by proper selection of the period $l_g = l_c$. Figure 8 reveals a severe deviation from the expected square dependence of the SH intensity with length. Evaluation of the apparent mismatch shown in Fig. 7 results in a deviation of 2.7% between l_g and l_c. In fact, the value of $l_c^{(e)} = 188$ μm has been obtained by ablation of the waveguide covered with the adsorbate, and hence does not take into account the coherence length of the actual device with a periodic modulation of the thickness of the waveguide by the coverage grating. It should be noted that shortening l_g by 2.7% approaches the theoretically expected value for l_c of 174 μm, according to Table I for the example of a $TM_0^{(\omega)} \rightarrow TM_2^{(2\omega)}$ conversion—which is, however, 7.5% off the experimental value $l_c^{(e)}$.

V. CONCLUSIONS

For the first time, to our knowledge, we have demonstrated second-harmonic generation using a planar waveguide covered with a nonlinear organic thin film. Quasi-phase-matching was achieved *in situ* by periodic modulation of this adsorbate in an *in situ* setup. Due to the physical dimensions of the commercial waveguide and the applied susceptibility, the conversion efficiency was rather low. It could, however, be shown that even nonoptimized quasi-phase-matched operation along a 3.8-mm device length—with 20 grating periods—resulted in an increase in efficiency of the selected $TM_0^{(\omega)} \rightarrow TM_2^{(2\omega)}$ mode pair by two orders of magnitude. By exploiting thin-film coverages prepared from Langmuir-Blodgett-type monolayers of high second-order nonlinearity ($\chi_S^{(2)} \approx 10^{-12}$ esu according to Ref. 22), one can expect conversion efficiencies in a percent range discussed in detail in Ref. 9. Another approach could be the use of recently available extremely thin (waveguide thickness 100 nm) metal-oxide waveguides, which can strongly enhance evanescent field interaction.

*Present address: Laser Laboratorium Göttingen e.V., Hans-Adolf-Krebs-Weg 1, D-37077 Göttingen, Germany.

[1] *Guided-Wave Nonlinear Optics,* edited by D. B. Ostrowsky and R. Reinisch (Kluwer Academic, Dordrecht, 1992), and references therein.

[2] D. B. Anderson and J. T. Boyd, Appl. Phys. Lett. **19**, 266 (1971).

[3] G. I. Stegeman and C. T. Seaton, Appl. Phys. **58**, R57 (1985).

[4] G. I. Stegeman, R. Zanoni, N. Finlayson, E. M. Wright, and C. T. Seaton, IEEE J. Lightwave Technol. **6**, 953 (1988).

[5] Y. R. Shen, *The Principles of Nonlinear Optics* (Wiley, New York, 1984).

[6] A. Okada, K. Ishi, K. Mito, and K. Sasaki, Nonlinear Opt. **1**, 179 (1991).

[7] K. O. Hill, A. Watanabe, and J. G. Chambers, Appl. Opt. **11**, 1952 (1972).

[8] A. Watanabe, K. O. Hill, and R. I. MacDonald, Can. J. Phys. **51**, 761 (1972).

[9] A. Bratz, B. U. Felderhof, and G. Marowsky, Appl. Phys. B **50**, 393 (1990).

[10] I. Ledoux, D. Josse, P. Vidakovic, and J. Zyss, Opt. Eng. **25**, 202 (1986).

[11] C. Bosshard, M. Flörsheimer, M. Küpfer, and P. Günter, Opt. Commun. **85**, 247 (1991).

[12] K. Iizuka, *Engineering Optics,* 2nd ed. (Springer-Verlag, Berlin, 1987); *Guided-Wave Optoelectronics,* edited by Theodor Tamir (Springer-Verlag, Berlin, 1988).

[13] H. A. Haus and G. A. Reider, Appl. Phys. **26**, 4576 (1987).

[14] F. Sieverdes, Ph. D. dissertation, University of Göttingen, 1992.

[15] H. P. Preiswerk, D. Neuschäfer, H. Spahni, G. Marowsky, M. Pinnow, F. Sieverdes, and A. Bratz, J. Opt. Soc. Am. B (to be published).

[16] T. F. Heinz, Ph.D. thesis, University of Berkeley, California, 1982.

[17] Cf. Equation 16.5-9 on page 394 in Amnon Yariv, *Quantum Electronics,* 3rd ed. (Wiley, New York, 1988).

[18] S. Lehmann, G. Marowsky, D. Neuschäfer, and H. Hsiung, Opt. Lett. (to be published).

[19] IOT Entwicklungsgesellschaft für Integrierte Optik-Technologie mbH, P.O. Box 1252, D-6833 Waghäusel-Kirrlach, Germany.

[20] B. U. Felderhof, A. Bratz, G. Marowsky, O. Roders, and F. Sieverdes, J. Opt. Soc. Am. B (to be published).

[21] G. Marowsky, L. F. Chi, D. Möbius, R. Steinhoff, Y. R. Shen, D. Dorsch, and B. Rieger, Chem. Phys. Lett. **147**, 420 (1988).

[22] G. Marowsky, M. Pinnow, F. Sieverdes, and E. Heinemann, Mol. Eng. **1**, 179 (1991).

[23] P. D. Maker, R. W. Terhune, M. Nisenoff, and C. M. Savage, Phys. Rev. Lett. **8**, 21 (1962).